

# Experimental Results on Multiple-Input Single-Output (MISO) Time Reversal for UWB Systems in an Office Environment

Chenming Zhou, *Student Member, IEEE*, Nan Guo, *Member, IEEE*, and Robert C. Qiu, *Senior Member, IEEE*

**Abstract**—This paper experimentally investigates the scheme of time reversal (TR) combined with multiple-input single-output (MISO) antennas over ultra-wideband (UWB) channels. In particular, temporal and spatial focusing as well as array gain are studied based on a  $(4 \times 1)$  MISO scheme in an office environment. The results confirm that the energy of UWB signals in an MISO scheme is more spatial-temporally focused than in a single-input single-output (SISO) scheme. As a result, a strong peak is observed in the equivalent channel impulse response. The magnitude of this peak grows linearly with the square root of the number of antenna elements at the transmitter. All the measurements and data processing are completed in the time domain.

**Index Terms**—Time reversal, UWB, MISO, spatial focusing, temporal focusing.

## I. INTRODUCTION

Ultra-wideband (UWB) transmission has recently received significant attention in both academia and industry for applications in short to medium range wireless communications [1] [2] [3]. UWB techniques have many attractive characteristics, including high data rate, low-cost, and low power consumption. However, there are a number of challenges in UWB receiver design, such as capturing multipath energy, reducing inter-symbol interference (ISI) and co-channel interference. A Time-Reversal (TR) technique has been applied to deal with these problems [4].

The process of TR technique includes two steps. First, the intended receiver sounds the channel by sending a short pulse to the transmitter. Second, the transmitter records, time-reverses and then retransmits the time reversed signal back to the channel. As a result, the energy will be focused in both the time and the space at the intended receiver. TR has been studied for a long time in acoustics [5] and extended to wireless communication recently [6].

Time reversal combining with antenna array at the transmitter (MISO-TR) seems to be a natural idea and has gained growing attention recently. Some measurements, e.g., the work in [7] [8], have been developed to investigate the spatial focusing and temporal focusing of the MISO-TR system. However, most of the work is done in narrowband and in outdoor

environments. Noticing the fundamental differences between the wideband channels and the narrowband channels, we carry out a series of measurements with UWB signals. Moreover, due to the wideband characteristic of UWB signals, time domain approach appears to be a better framework to study the radiation, propagation, and reception of the UWB systems. We conduct the measurements and the data processing directly in the time domain, which is another feature distinguishing our work from most of the previous work.

Our contributions in this paper are trifold. First, we experimentally demonstrate that the UWB transmission range could be extended by employing multiple antennas at the transmitter. It is found that the peak energy at the receiver increases linearly with the number of antennas employed in the transmit array. Part of the experimental results are reported in [9], and this paper gives the mathematical proof. Second, we demonstrate very good spatial focusing of the MISO-TR systems. A comparison is made between Single Input and Single Output Time Reversal (SISO-TR) and MISO-TR, and the results show that the MISO-TR increases the spatial focusing by several decibels, compared with the SISO-TR. Finally, a detailed comparison of the temporal focusing for MISO-TR, SISO-TR, and the original channel without TR scenarios is provided, confirming that MISO-TR can further temporally compress the channel.

The remainder of this paper is organized as follows: In Section II, we analyze the array gain of the MISO-TR system. Some formulations that will be used in this paper are also introduced. We give detailed experiment description, including experiment setup and experiment environment in Section III. The measurement results and the corresponding analysis are shown in Section IV. Finally, conclusions are drawn in Section V.

## II. UWB MISO TR SYSTEM

### A. Impulse MISO

A  $4 \times 1$  MISO-TR system configuration is illustrated in Fig. 1. Let  $h_m(t)$  denote the channel impulse response (CIR) between the  $m$ -th element of the transmit array and the receiver, and  $c_m(t)$  be the corresponding prefilter code employed in that antenna branch. In a TR system, the conjugate of the CIR will be used as the prefilter of that channel. Thus, we have

$$c_m(t) = A_m h_m(-t) \quad (1)$$

This work is funded in part by the Army Research Laboratory and the Army Research Office through a STIR grant (W911NF-05-1-0468) and a DURIP grant (W911NF-05-1-0111).

Chenming Zhou, Nan Guo and Robert C. Qiu are with the Center for Manufacturing Research, Department of Electrical and Computer Engineering, Tennessee Technological University, Cookeville, TN 38505. Email: {czhou21, nguo, rqi} @tntech.edu

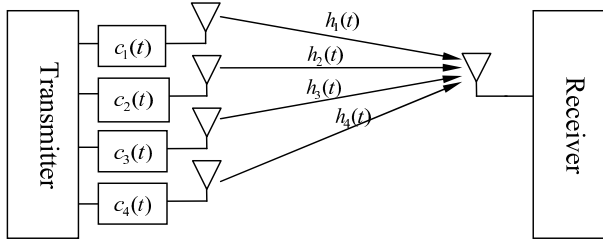


Fig. 1. Time reversal precoded MISO communication systems with  $M=4$  transmit antennas and one receive antenna.

where  $A_m$  is the power scaling factor that describes various power allocation situations [8]. Notice that the transmit power is normalized by utilizing the power scaling factor  $A_m$  [8].

Generally, one uses channel sounding to get the CIR  $h_m(t)$ . Let  $p(t)$  denote the sounding pulse sent by the receiver, and  $q(t)$  be the signal received by the transmitter. Then it follows that,  $q(t) = p(t) * h(t)$ , where  $h(t)$  is the CIR, and  $*$  denotes convolution operation. The transmitter directly samples  $q(t)$  and uses the complex conjugate of  $q(t)$  as the prefilter. In the next step, the transmitter sends the same pulse  $p(t)$  (or a modulated pulse) to the receiver, and the receiving signal would be

$$\begin{aligned} r(t) &= p(t) * q(-t) * h(t) \\ &= R_{pp}(t) * R_{hh}(t) \end{aligned} \quad (2)$$

where  $R_{pp}(t)$  and  $R_{hh}(t)$  are the autocorrelation of the  $p(t)$  and  $h(t)$ , respectively.

Note that noise term has been ignored in (2) for the sake of simplicity. Traditionally,  $h(-t)$ , instead of  $q(-t)$ , is applied as the prefilter code. Then the received signal is described by  $r(t) = p(t) * R_{hh}(t)$ . Often  $R_{pp}(t)$  is sharper than  $p(t)$ , especially when we use a chirp pulse as the sounding pulse  $p(t)$ . Under this condition,  $R_{pp}(t)$  will approach the delta function by choosing proper parameters. Thus, from (2) it follows that

$$r(t) \approx R_{hh}(t) \quad (3)$$

It is known that a short UWB pulse signal, by its nature, is impulsive and transient. The limit of a UWB signal is the Dirac pulse of zero duration, but of infinite bandwidth. The interest in this paper is to study the limit of MISO in the context of TR. In the following time domain measurements, we will first use the CLEAN algorithm [10] [11] to extract the impulse response from the received waveforms. Later on all of the analysis will be based on the CIRs.

## B. Array Gain

Array Gain is the gain achieved by using multiple antennas so that the signal adds coherently. This section will illustrate, by employing MISO-TR technique, how the peaks of the signal at the receiver are automatically aligned and an array gain factor of  $M$  (the number of antenna elements at the transmitter) over the SISO is achieved.

For equal power allocation [8], we have

$$A_m = \frac{1}{\sqrt{M} \sqrt{\|h_m(t)\|^2}} \quad (4)$$

where “ $\| \cdot \|$ ” denotes the Frobenius norm operation defined as:  $\|x(t)\|^2 = \int_{-\infty}^{+\infty} |x(t)|^2 dt$ .

The equivalent impulse response can be expressed as

$$h_{eq}(t) = \sum_{m=1}^M c_m(t) * h_m(t) \quad (5)$$

It should be noted that, in reality, time can not be truly reversed to obtain the reversed CIR  $h_m(-t)$  in (1). Therefore, a FIR filter with a length of  $T$  is always required to implement the time reverse operation. This will lead an expression of  $h_m(T-t)$ , instead of  $h_m(-t)$ , in (1). The filter length  $T$  should be chosen to be bigger than the maximum delay spread of all of the CIRs.

For the MISO case we have

$$\begin{aligned} h_{eq}^{MISO}(t) &= \sum_{m=1}^M \frac{1}{\sqrt{M} \sqrt{\|h_m(t)\|^2}} h_m^*(T-t) * h_m(t) \\ &= \sum_{m=1}^M \frac{1}{\sqrt{M} \sqrt{\|h_m(t)\|^2}} R_{h_m h_m}(t) * \delta(t-T) \end{aligned} \quad (6)$$

where  $R_{h_m h_m}(t)$  is the autocorrelation of  $h_m(t)$ .

As a special case when  $M=1$ , which corresponds to a SISO scenario, it follows that

$$\begin{aligned} h_{eq}^{SISO}(t) &= \frac{1}{\sqrt{\|h_1(t)\|^2}} h_1^*(T-t) * h_1(t) \\ &= \frac{1}{\sqrt{\|h_1(t)\|^2}} R_{h_1 h_1}(t) * \delta(t-T) \end{aligned} \quad (7)$$

Notice that a sharp peak will usually be generated in the equivalent CIR, due to the temporal focusing of the TR technique. Most of the time we may only need a simple receiver to pick up the peak energy of the impulse response. Therefore, our focus will be on the peak.

It is known that the peak of the autocorrelation  $R_{h_m h_m}(t)$  occurs at the instant  $t=0$  with a magnitude equal to the energy of  $h_m(t)$ . Mathematically, it follows that,  $R_{h_m h_m}(0) = \|h_m(t)\|^2$ . If the same initial timing between antenna elements is assumed (this is reasonable assumption because all the antenna elements at the transmitter are using the same clock), then all the peaks of the fields in (6) reach at the same time instant  $T$  independent of the element location, antenna type and channel [12]. It seems like that the peaks are aligned automatically.

For the MISO case, all the energies from different elements coherently add up at time  $T$ . It follows from (6) that

$$\begin{aligned} h_{eq}^{MISO}(T) &= \sum_{m=1}^M \frac{1}{\sqrt{M} \sqrt{\|h_m(t)\|^2}} R_{h_m h_m}(0) \\ &= \sum_{m=1}^M \frac{1}{\sqrt{M}} \sqrt{\|h_m(t)\|^2} \end{aligned} \quad (8)$$

For the SISO case, it follows from (7) that

$$h_{eq}^{SISO}(T) = \sqrt{\|h_m(t)\|^2} \quad (9)$$

Let  $\mu = \frac{1}{M} \sum_{m=1}^M \sqrt{\|h_m(t)\|^2}$ , where  $\mu$  represents the average peak height over all the  $M$  TR channels. Eq. (8) is reduced to

$$\begin{aligned} h_{eq}^{MISO}(T) &= \sum_{m=1}^M \frac{1}{\sqrt{M}} \sqrt{\|h_m(t)\|^2} \\ &= \sqrt{M} \mu \end{aligned} \quad (10)$$

Eq. (10) can be physically interpreted as: the peak in the equivalent CIR of MISO case is  $\sqrt{M}$  higher than the peak

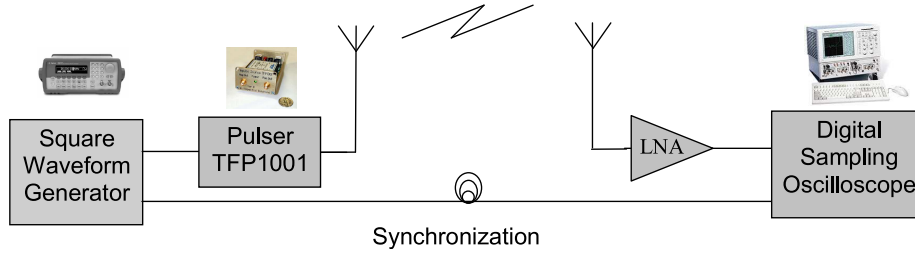


Fig. 2. Experiment setup

average over all the  $M$  SISO cases. In terms of energy, by using MISO of  $M$  elements an array gain factor of  $M$  over the SISO can be achieved. This result is inspired by the maximum radio combining (MRC) in the narrowband MISO array.

### C. Spatial Focusing

Let  $h(\mathbf{r}_0, t)$  represent the CIR for the intended receiver located in the position  $\mathbf{r}_0(x_0, y_0, z_0)$ , and  $h(\mathbf{r}_1, t)$  denote the CIR of another unintended user at the position  $\mathbf{r}_1$ . The equivalent CIR for the intended user would be

$$h_{eq}(\mathbf{r}_0, \mathbf{r}_0, t) = h(\mathbf{r}_0, -t) * h(\mathbf{r}_0, t) \quad (11)$$

For the unintended user, the equivalent CIR would be

$$h_{eq}(\mathbf{r}_0, \mathbf{r}_1, t) = h(\mathbf{r}_0, -t) * h(\mathbf{r}_1, t) \quad (12)$$

The spatial focusing can be characterized by the metric directivity  $D(\mathbf{r}_0, \mathbf{r}_1)$  defined as

$$D(\mathbf{r}_0, \mathbf{r}_1) = \frac{\max_t |h_{eq}(\mathbf{r}_0, \mathbf{r}_0, t)|^2}{\max_t |h_{eq}(\mathbf{r}_0, \mathbf{r}_1, t)|^2} \quad (13)$$

For the MISO-TR case, the equivalent CIR for different users can be expressed as

$$\begin{aligned} h_{eq}(\mathbf{r}_0, \mathbf{r}_0, t) &= \sum_{m=1}^M \frac{1}{\sqrt{M} \sqrt{\|h_m(\mathbf{r}_0, t)\|^2}} h_m(\mathbf{r}_0, -t) * h_m(\mathbf{r}_0, t) \\ h_{eq}(\mathbf{r}_0, \mathbf{r}_1, t) &= \sum_{m=1}^M \frac{1}{\sqrt{M} \sqrt{\|h_m(\mathbf{r}_0, t)\|^2}} h_m(\mathbf{r}_0, -t) * h_m(\mathbf{r}_1, t) \end{aligned} \quad (14)$$

where  $h_m(\mathbf{r}_0, t)$  denotes the CIR between the  $m$ -th element in the transmit array and the receiver located in  $\mathbf{r}_0$ .

Note that for simplicity, the receiver is restricted to move along a line in the measurements carried out in this paper. Under this condition, Eq. (13) can be simplified as

$$D(\mathbf{r}_0, d) = \frac{\max_t |h_{eq}(\mathbf{r}_0, 0, t)|^2}{\max_t |h_{eq}(\mathbf{r}_0, d, t)|^2} \quad (15)$$

where  $d$  is the distance between the unintended receiver and the intended receiver (focal point) located at  $\mathbf{r}_0$ . For the case where the antenna elements are not distributed along a line, but in some shapes (e.g., circle, square and etc.), (15) will be still valid by replacing the scalar  $d$  with a vector  $\mathbf{d}$ , where  $\mathbf{d} = \mathbf{r}_1 - \mathbf{r}_0$ .

The value of directivity  $D(\mathbf{r}_0, d)$  determines how well we can, by employing TR, focus the transmitted energy into an intended point of interest. A similar metric has been used in [13].

Our previous paper [15] uses the same metric to investigate the spatial focusing of the UWB signal in the hallway environment by simulation. In this paper, we will experimentally investigate this parameter by moving the receiver away from the intended focusing point,  $\mathbf{r}_0$ , and studying how rapidly the receiving energy will drop with this moving.

### D. Temporal Focusing

One of the metrics to characterize the temporal dispersion of a radio channel is the Root Mean Square (RMS) delay spread, which is the square root of the second central moment of the power delay profile. Mathematically, RMS delay spread  $\tau_{rms}$  can be expressed as:

$$\tau_{rms} = \left[ \frac{\int_{-\infty}^{\infty} (t - \tau_m)^2 |h(t)|^2 dt}{\|h(t)\|^2} \right]^{1/2} \quad (16)$$

where

$$\tau_m = \frac{\int_{-\infty}^{\infty} t |h(t)|^2 dt}{\|h(t)\|^2} \quad (17)$$

is the mean excess delay spread of the channel. RMS delay spread is one of the most important parameters for system design since it is closely related to the inter-symbol interference (ISI).

Another metric of interest to measure temporal focusing is the peak to sidelobe energy ratio, defined as the ratio of the energy in the main peak to the rest of the impulse response. Mathematically, the peak to sidelobe energy ratio  $\eta$  is expressed as

$$\eta = \frac{\max_t |h_{eq}(t)|^2}{\|h_{eq}(t)\|^2 / dt - \max_t |h_{eq}(t)|^2} \quad (18)$$

The metric  $\eta$  defined in this paper is similar to the temporal compression ratio defined in [4] and the temporal energy ratio in [14].

## III. MEASUREMENT

### A. Experiment Setup

A simplified block diagram of the experiment setup is shown in Fig. 2. Major equipment used in the measurements includes: (1) a waveform generator for triggering the pulser, (2) a UWB pulser that generates Gaussian like pulses with RMS pulse width of approximate 250 ps, (3) a wideband low noise amplifier (LNA) with bandwidth over 10 GHz and noise figure

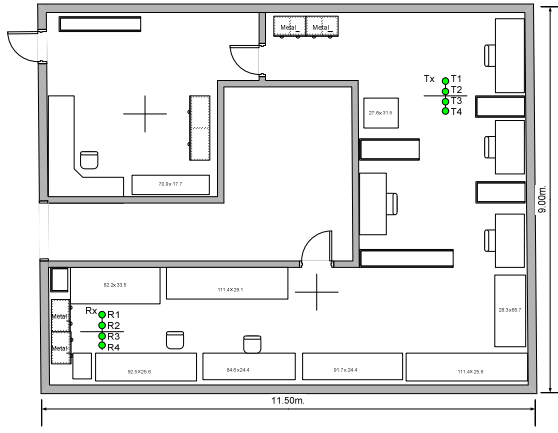


Fig. 3. Experiment environment

less than 1.5 dB, (4) a Tektronix CSA8000 Digital Sampling Oscilloscope (DSO) with a 20 GHz sampling module 80E03, and (5) a pair of omni-directional antennas with relatively flat gain over the signal band. To maintain synchronization, the same waveform generator is employed to trigger the DSO. The major frequency components of the system are from 750MHz to 1.6GH.

A virtual antenna array is employed in the experiments. The elements of the array are spaced far enough such that there is no coupling between them. This can be achieved if the spacings between any two adjacent antenna elements are greater than 20 cm, which corresponds to the half wavelength of the lowest frequency. The value of 20 cm is found to be sufficient after some trials of bigger values. In Fig. 3, four virtual elements are equally spaced along a line. The heights of antennas are set to 1.4 m. The receiving antenna is moved to different locations, and individual channel was sounded and measured sequentially. No Line of Sight (LOS) is available for all the measurements.

### B. Experiment Environment

A set of measurements have been developed in the office area of Clement Hall 400 at Tennessee Technological University. Fig. 3 shows the experimental layout for these experiments. The environment for the experiment is a typical office area with abundance of wooden and metallic furniture (chairs, desks, bookshelves and cabinets).

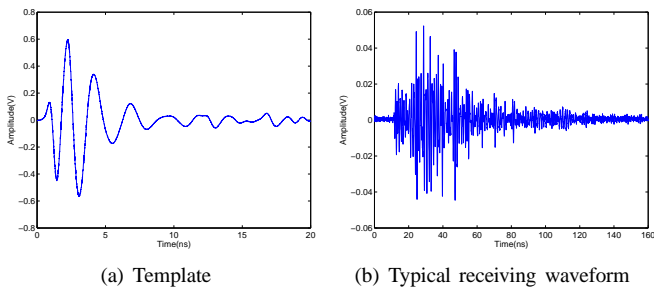


Fig. 4. 1 meter template for CLEAN algorithm and a typical receiving waveform in an office environment.

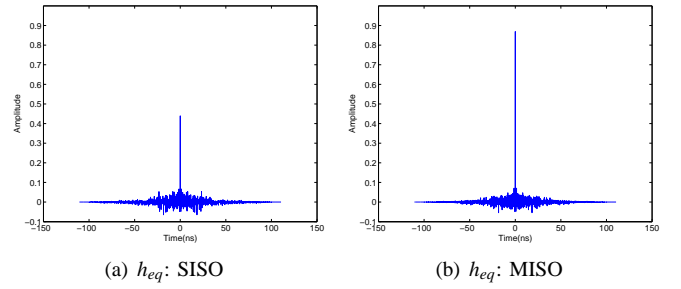


Fig. 5. Comparison of the equivalent CIRs for different scenarios: SISO and MISO

## IV. MEASUREMENT RESULTS AND ANALYSIS

A typical receiving waveform is shown in Fig. 4(b). Let  $T_n$  denote the  $n$ -th element of the transmitting array and  $R_n$  the receiver located in  $n$ -th position. Fig. 4(b) shows the receiving waveform for the channel between  $T_2$  and  $R_4$ . The CLEAN algorithm is employed to extract CIR from the receiving waveform. The template used in the CLEAN algorithm is shown in Fig. 4(a).

### A. Array Gain

In this section, we investigate the array gain by comparing the peak power in the equivalent CIRs of SISO-TR and MISO-TR systems. The equivalent CIRs for different scenarios are shown in Fig. 5. Fig. 5(a) is for SISO-TR case between  $T_2$  and  $R_4$ . The equivalent CIR for SISO-TR is calculated by (7). Fig. 5(b) is for MISO-TR case with  $T_{1,2,3,4}$  as the transmitter array and  $R_4$  the receiver. The equivalent CIR for MISO-TR is calculated by (6). It is observed that the peak in Fig. 5(b) is about two times higher than that in Fig. 5(a). We then further calculate the average peak height of all the four SISO cases ( $T_1R_4, T_2R_4, T_3R_4, T_4R_4$ ). The results confirm the conclusion obtained in section II(B) that the peak of the CIR for the MISO is  $\sqrt{M}$  times higher than that of the SISO. The higher peak in the equivalent CIR corresponds to a stronger signal that could be captured by the receiver. Noticing that the transmitting power for MISO and SISO cases have been set to be identical according to (4), therefore the MISO-TR technique greatly improves the power efficiency of the system. Since the propagation distance is limited by the low transmitting power for a UWB system, MISO-TR could be an effective solution used for UWB range extension.

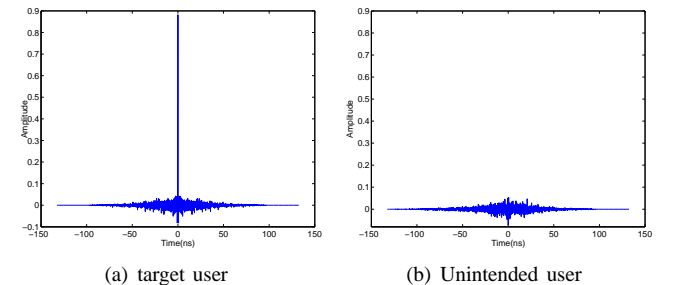


Fig. 6. Demonstration of MISO-TR spatial focusing by the equivalent CIR. (a) is the equivalent CIR of the target user. (b) is the equivalent CIR of the unintended user with 0.2m away from the target user.

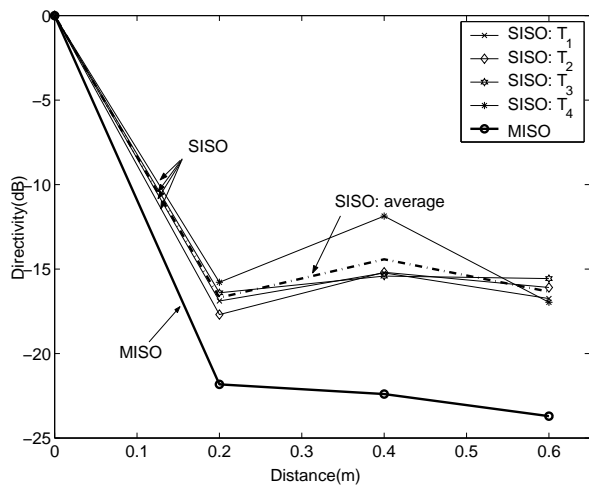


Fig. 7. Spatial focusing characterized by the parameter directivity.

### B. Spatial Focusing

We first investigate the spatial focusing of a MISO-TR system. Consider downlink transmission. Assume there are two users separated by a distance  $d$ , with one of them as the target user (focal point) and the other one as the undesired user. Each user has one receive antenna and shares the same transmit array with four elements. The equivalent CIRs for the target user and the undesired user of  $0.2m$  away are shown in Fig. 6(a) and Fig. 6(b), respectively. The equivalent CIRs for different kinds of users are calculated by using (14). As we can see from Fig. 6, the signal is very strong for the target user while it is almost behind the background noise for the undesired user with a short distance of  $0.2m$  away.

We further investigate the variation of parameter directivity  $D$ , defined in section II(C), with respect to different distances  $d$ . A comparison of spatial focusing for MISO-TR and SISO-TR is shown in Fig. 7. In the SISO-TR case, it is observed that more than  $15dB$  energy drops when the undesired receiver is located  $0.2m$  away from the intended user. This number will slightly change when the unintended receiver moves to a farther place. In Fig. 7, the “SISO average” curve represents the average directivity of the four SISO-TR cases. It is observed that the “MISO” directivity curve drops much faster than the “SISO average” curve, implying that spatial focusing is improved by employing antenna array at the transmitter. With a 4 element array at the transmitter,  $22dB$  energy drops when the unintended receiver is  $0.2m$  away from the target receiver.

### C. Temporal Focusing

As illustrated in Fig. 3, we use a  $4 \times 4$  MIMO (multiple-input, multiple-output) virtual array, corresponding to 16 SISO channels, or 4 sets of MISO ( $4 \times 1$ ) channels. Fig. 8 shows a comparison of RMS delay for different scenarios. The curve labeled by “Original Channel” gives the RMS delay spreads for all the 16 channels, assuming neither antenna array nor time reversal technique is involved. Then we apply TR technique on these 16 channels, respectively, and their

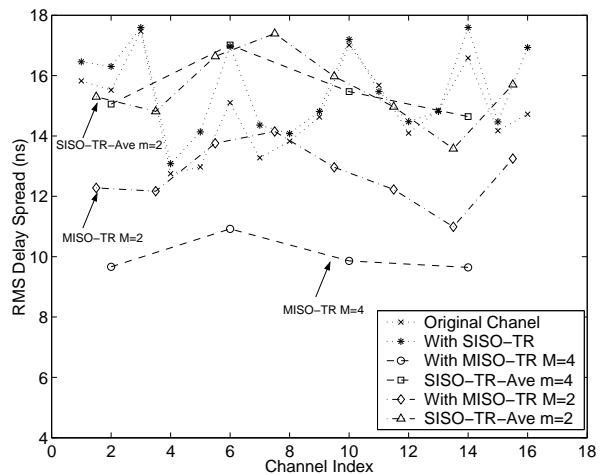


Fig. 8. Demonstration of MISO-TR temporal focusing by RMS delay spread.

corresponding equivalent RMS delay spreads are shown in the curve labeled by “With SISO-TR”.

It is interesting to notice that TR alone will not reduce the RMS delay spread, as we can see when we compare the “original channel” curve and the “With SISO-TR” curve. The reason why TR alone does not reduce the RMS delay spread is that the length of the equivalent CIR, after an autocorrelation operation, is almost doubled. The additional length of the channel contributes to the calculation of the delay spread.

Four SISO-TR channels sharing the same receive antenna are chosen to form a  $4 \times 1$  MISO-TR channel. Totally we have 4 sets of  $4 \times 1$  MISO-TR channels, with their equivalent RMS delay spreads described by the curve labeled by “With MISO-TR M=4”. As a reference, the average RMS delay spreads over these four SISO-TR channels are calculated and shown in the curve labeled by “SISO-TR-Ave m=4”. It is apparent that the RMS delays in the “With MISO-TR M=4” curve are much smaller than that in the “SISO-TR-Ave m=4” curve, indicating that the RMS delay spread is greatly reduced by employing multiple antennas at the transmitter.

To study the impact of the element number in an MISO-TR channel on the RMS delay spread reduction, we repeat the above processing by forming  $2 \times 1$  MISO-TR channels with the two channels sharing the same receiver. The corresponding RMS delay spreads are shown by the curve “With MISO-TR M=2” and “SISO-TR-Ave m=2”, respectively. It is observed that RMS delay spread reduction is closely related to the number of elements at the transmitter array and is almost doubled when we increase the number of elements from 2 to 4.

Under certain circumstances we are more interested in the peak energy, e.g., in the case that a simple receiver such as directly thresholding is used. Fig. 9 gives a comparison of the peak to sidelobe energy ratios,  $\eta$ , for different scenarios. A comparison between the “original channel” curve and the “SISO-TR” curve shows that, though unable to reduce RMS delay spread, TR does temporally compress the channel in the sense that it increases the value of  $\eta$ . As shown in Fig. 9, MISO-TR can further increase the value of  $\eta$  to

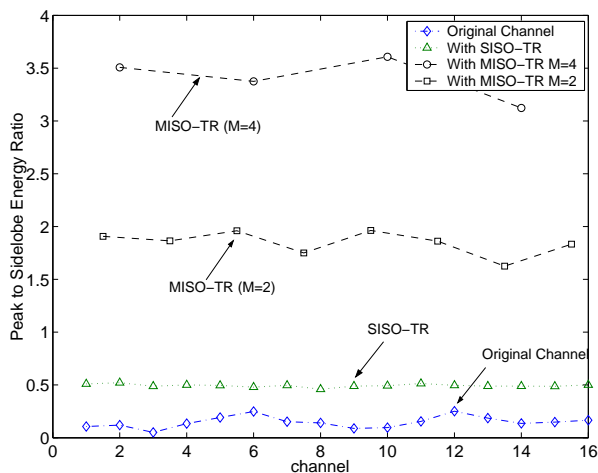


Fig. 9. Demonstration of MISO-TR temporal focusing by peak to sidelobe energy ratio.

some extent, depending on the number of elements at the transmitter. For example, for a SISO-TR channel, the value of  $\eta$  is about 0.5. This number is increased to, roughly, 1.9 and 3.5, by employing an antenna array with 2 and 4 elements, respectively. The highly temporal focusing provided by an MISO-TR scheme (e.g., for a  $4 \times 1$  MISO-TR, eighty percent of the energy is focused in the main peak) will significantly reduce the task of equalization and energy collection and hence the complexity of the receiver.

We repeat the experiments by moving the receiver array (virtual array) to different locations (marked in Fig. 3 by cross lines) in the office. Similar conclusions are obtained from different locations.

## V. CONCLUSION

It is known that time reversal technique provides spatial focusing as well as temporal focusing. In this paper, we experimentally show that these two characteristics can be further improved by employing multiple antennas at the transmitter. A series of measurements are carried out in an office environment with UWB signals. All the measurements and data processing are done in the time domain. It is also shown that the peak power in the equivalent impulse response of the MISO-TR scheme increases linearly with the number of the antennas employed at the transmitter. Therefore, MISO-TR could be a good solution to extend the transmission range of UWB systems.

The excellent spatial focusing characteristic provided by MISO-TR hints at a significant advantage for parallel information transmission when multiple antennas are employed at

both ends (MIMO-TR). UWB MIMO-TR [16] is a promising topic, and more work needs to be done in the future.

## VI. ACKNOWLEDGMENTS

The authors want to thank Drs. Brian Sadler, Robert Ulman, T. C. Yang, and Santanu Das for their useful discussions. Special thanks to those anonymous reviewers for their valuable comments, which help improve this paper.

## REFERENCES

- [1] R. A. Scholtz, "Multiple access with time-hopping impulse modulator (invited paper)," *MILCOM'93*, Bedford, Massachusetts, October 11-14, 1993.
- [2] M. Z. Win and R. A. Scholtz, "Characterization of ultra-wide bandwidth wireless indoor communications channel: A communication theoretic view," *IEEE J. Select. Areas Commun.*, vol. 20, no. 9, pp. 1613-1627, Dec. 2002.
- [3] D. Porcino and W. Hirt, "Ultra-wideband radio technology: potential and challenges Ahead," *IEEE Commun. Mag.*, Vol. 41, No. 7, pp. 66-74, 2003.
- [4] T. Strohmer, M. Emami, J. Hansen, G. Papanicolaou, A. J. Paulraj, "Application of time-reversal with MMSE equalizer to UWB communications," *Proc. IEEE Global Telecommunications Conference*, vol.5 pp. 3123-3127, 2004.
- [5] M. Fink, "Time reversed acoustics," *Physics Today*, pp. 34-40, Mar. 1997.
- [6] C. Oestges, *et al.*, "Characterization of space-time focusing in time-reversed random fields," *IEEE Trans. On Antennas and Propagat.*, Vol. 53, No. 1, pp. 283-293, Jan. 2005.
- [7] H. T. Nguyen, J.B. Andersen, G. G. Pedersen, "The potential use of time reversal techniques in multiple element antenna systems," *IEEE Communication Letters*, vol. 9, No. 1, pp. 40-42. Jan. 2005.
- [8] P. Kyristi, G. Papanicolaou, A. Oprea, "MISO time reversal and delay-spread compression for FWA channels at 5 GHz," *IEEE Antennas And Wireless Propagation Letters*, vol. 3, pp. 96-99, Dec. 2004.
- [9] R. C. Qiu, C. Zhou, N. Guo, J. Q. Zhang, "Time reversal with MISO for Ultra-Wideband communications: experimental results," *IEEE Antennas and Wireless Propagation Letters*, pp. 269-273, Vol. 5, 2006.
- [10] R. J. Cramer, "An evaluation of ultrawideband propagation channels," *PhD Dissertation*, University of Southern California, California, USA. Dec. 2000.
- [11] R. M. Buehrer and *et al.*, "Ultra-wdeband propagation measurements and modeling final report," *DARPA NETEX program*, pp. 333- , Virginia Polytechnic Institute and State University, VA, USA. Jan. 2004.
- [12] M. Fink, "Time reversal of ultrasonic fields-part I: basic principle," *IEEE Trans. Ultrason., Ferroelectr. Freq. Control*, Vol. 39, pp. 555-566, Sept. 1992.
- [13] S. M. Emami, J. Hansen, A. D. Kim, G. Papanicolaou, A. J. Paulraj, D. Cheung, and C. Prettie, "Predicted time reversal performance in wireless communications using channel measurements," *IEEE communication letters*, to appear, 2004.
- [14] R. Daniels and R. Heath, "Improving on time reversal with MISO precoding," *Proceedings of the Eighth International Symposium on Wireless Personal Communications Conference*, Aalborg, Denmark, September 18-22, 2005.
- [15] C. Zhou and R. C. Qiu, "Spatial focusing of time-reversed UWB electromagnetic waves in a hallway environment," Submitted to *IEEE 38th Southeastern Symposium on System Theory*, Cookeville, TN, USA. March 5-7, 2006.
- [16] R. C. Qiu, "A Theory of Time-Reversed Impulse Multiple-Input Multiple-Output (MIMO) for Ultra-Wideband (UWB) Communications," invited paper, *IEEE International Conf. Ultra Wideband (ICUWB06)*, Boston, MA, Sept. 2006.